ISSN 1569-1713, Volume 6, Number 3

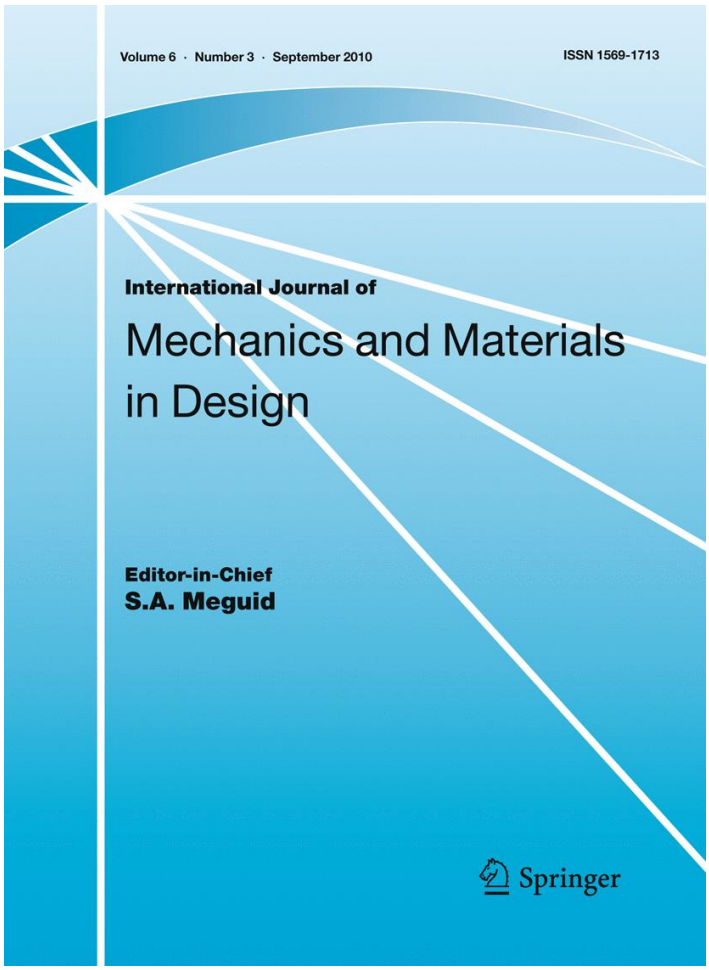

Int J Mech Mater Des (2010) 6:269–282
DOI 10.1007/s10999-010-9136-0

On deformation of functionally graded narrow beams under transverse loads

Sandeep S. Pendhari · Tarun Kant · Yogesh M. Desai · C. Venkata Subbaiah

Received: 12 April 2010 / Accepted: 27 August 2010 / Published online: 17 September 2010

Abstract Solution is obtained for functionally graded (FG) narrow beams under plane stress condition of elasticity by using the mixed semi analytical model developed by Kant et al. (Int J Comput Methods Eng Sci Mech 8(3): 165–177, 2007a). The mathematical model consists in defining a two-point boundary value problem (BVP) governed by a set of coupled first-order ordinary differential equations (ODEs) in the beam thickness direction. Analytical solutions based on two dimensional (2D) elasticity, one dimensional (1D) first order shear deformation theory (FOST) and a new 1D higher order shear-normal deformation theory (HOSNT) are also established to show the accuracy, simplicity and effectiveness of the developed mixed semi analytical model. It is observed from the numerical investigation that the present mixed semi analytical model predicts structural response as good as the one given by the elasticity analytical solution which in turn proves the robustness of the present development.

S. S. Pendhari (✉)
Engineering Department, Zentech India, 1st Floor, 5th Building, 2nd Sector, Millennium Business Park, Mahape, Navi Mumbai 400 710, India
e-mail: spendhari@zentech-usa.com

T. Kant · Y. M. Desai · C. Venkata Subbaiah
Department of Civil Engineering, Indian Institute of Technology Bombay, Mumbai 400 076, India

Keywords Mixed semi analytical method · FG beams · HOSNT · FOST · Plane stress

1 Introduction

Laminated composite/sandwich materials are being increasingly used in the aeronautical and aerospace industry as well as in other fields of modern technology. But, the main disadvantage of laminated composites is characterized by the weakness at interfaces. In the absence of any graded material at the interface, there is every chance of delamination to occur. To eliminate these interface problems, a new class of materials named functionally graded material (FGM) has recently been proposed whose physical properties vary through the thickness in a continuous manner and are therefore free from interface weaknesses typical of laminated composites. These advanced composite materials were first introduced by a group of scientists in Sendai (Japan) in 1984 (Yamanouchi et al. 1990, Koizumi 1993). Now, the concept of functionally graded (FG) has been widely employed in almost all engineering applications including electronics, aerospace, biomedicine, optics, etc.

Considerable work (Kant 1982; Kant et al. 1982; Reddy 2000; Kant and Manjunatha 1998; Vel and Batra 1999; Kant et al. 2007a, b) has been devoted to the development of computational (analytical and numerical) models for studying structural behavior

under transverse/thermal/electric loads. Three dimensional (3D) elasticity solutions based on the solution of partial differential equations (PDEs) with appropriate boundary conditions are valuable because they represent a more realistic and closer approximation to the actual behavior of the structures. Sankar (2001) has presented a 2D elasticity solution under plane strain condition for FG beams subjected to sinusoidal loads by assuming Young's modulus to vary exponentially through the thickness of beam. Further, Sankar and Tzeng (2002) extended the same elasticity solutions for a FG beams subjected to thermal loads.

Bian et al. (2005) extended the Soldatos and Liu (2001) plate theory for stress analysis of FG plate under cylindrical bending. Transfer matrix method (TMM) proposed by Thomson (1950) is used to derive the shape functions. TMM approach helps to improve the computational efficiency as compared to original model developed by Soldatos and Liu (2001). The shear stiffness and shear correction coefficients associated with first-order shear deformation theory were calculated by Nguyen et al. (2008) for FG simply supported plates under cylindrical bending. Matsunaga (2009) developed higher-order shear deformation model for evaluation of displacements and stresses in FG simply supported plates subjected to thermo-mechanical loads. Khabbaz et al. (2009) used energy concept along with the first and third order shear deformation theories to predict the large deformation and through thickness stress of FGM plates. Kang and Li (2009) studied non-linear behaviour of a cantilever beam subjected to an end force by using large and small deformation theories.

A finite element (FE) model based on FOST is developed by Chakraborty and Gopalakrishnan (2003a) to study the thermoelastic behavior of FG beam structures. The exact solution of static part of the governing differential equations is used in the formulation to construct interpolating polynomials which results in stiffness matrix having super-convergent property. Extension of the formulation to capture wave propagation behavior in a FG beam with high frequency impulse loading is also given by Chakraborty and Gopalakrishnan (2003b). Lee (2003) presented a mixed FE formulation to investigate the structural response of FG piezoelectric beams based on the linear thermo-piezoelectricity principles which accounts for the coupled mechanical, electrical and thermal response. Analytical solutions for piezoelectric FG half-spaces under uniform circular surface loading are presented by Han et al. (2006). The effect of different exponential factors of the FG materials on the field response is demonstrated in detail. The presented solutions are likely to be useful in the characterization of material properties for piezoelectric FG structures.

Woo and Meguid (2001) presented non-linear analytical solutions for the coupled large deflection of FG plates and shells under thermo-mechanical loading. The material properties of FGM are assumed to vary according to power-law distribution of the volume fraction of the constituents through the thickness. The fundamental equations are obtained using the von Karman theory for large deflection. Further, analytical solution is presented by Woo et al. (2005) for post-buckling analysis of moderately thick FG plates and shells under edge compression loads and a temperature field. Bodaghi and Saidi (2010) presented analytical approach based on a higher-order shear deformation theory to determine critical buckling loads of thick FG rectangular plates.

The meshless local Petrov–Galerkin (MLPG) method is a novel numerical approach. MLPG method allows the construction of the shape functions and domain discretization without defining elements. The use of MLPG approach to study transient thermoelastic response of FG composites heated by Gayssial laser beam is demonstrated by Ching and Chen (2006). Extensive parametric studies for transient and steady-state thermomechanical responses with respect to spatial distribution, volume fraction of material constituents, rate of laser power and radius of laser beam have been presented. Further, Sladek et al. (2005) has proposed MLPG approach for crack analysis in anisotropic FG materials for quasi-static and transient elastodynamic problems.

Taking a cue from foregoing developments, an effort is made in this paper to extend the mixed semi analytical formulation developed by Kant et al. (2007a) for stress analysis of simply (diaphragm) supported FG beam under transverse loads. 2D elasticity solution presented by Sankar (2001) is reformulated for plane stress condition. Details of this reformulation are omitted here for the sake of brevity. Readers are advised to refer Sankar (2001) for details. In addition to these, analytical solutions based on FOST and HOSNT are also developed and presented.

2 Formulations

A FG beam (Fig. 1) supported on two opposite edges, $x = 0$ and L, is considered. The length of beam is L and thickness is h. The beam is assumed to be in a state of 2D plane stress in x–z plane and width in the y direction is considered as unity. The top surface of the beam is subjected to only transverse loading which can be expressed as,

$$p(x) = \sum_m p_{0m} \sin \frac{m\pi x}{L} \tag{1}$$

where, $m = 1, 3, 5, \ldots\ldots$

The bottom surface is completely free of any stresses. In Eq. 1, m is assumed to be odd. The loading is symmetric about the center of beam and any arbitrary normal loading can be expressed with the help of Fourier series involving the terms of the type $p_{0m} \sin \frac{m\pi x}{L}$.

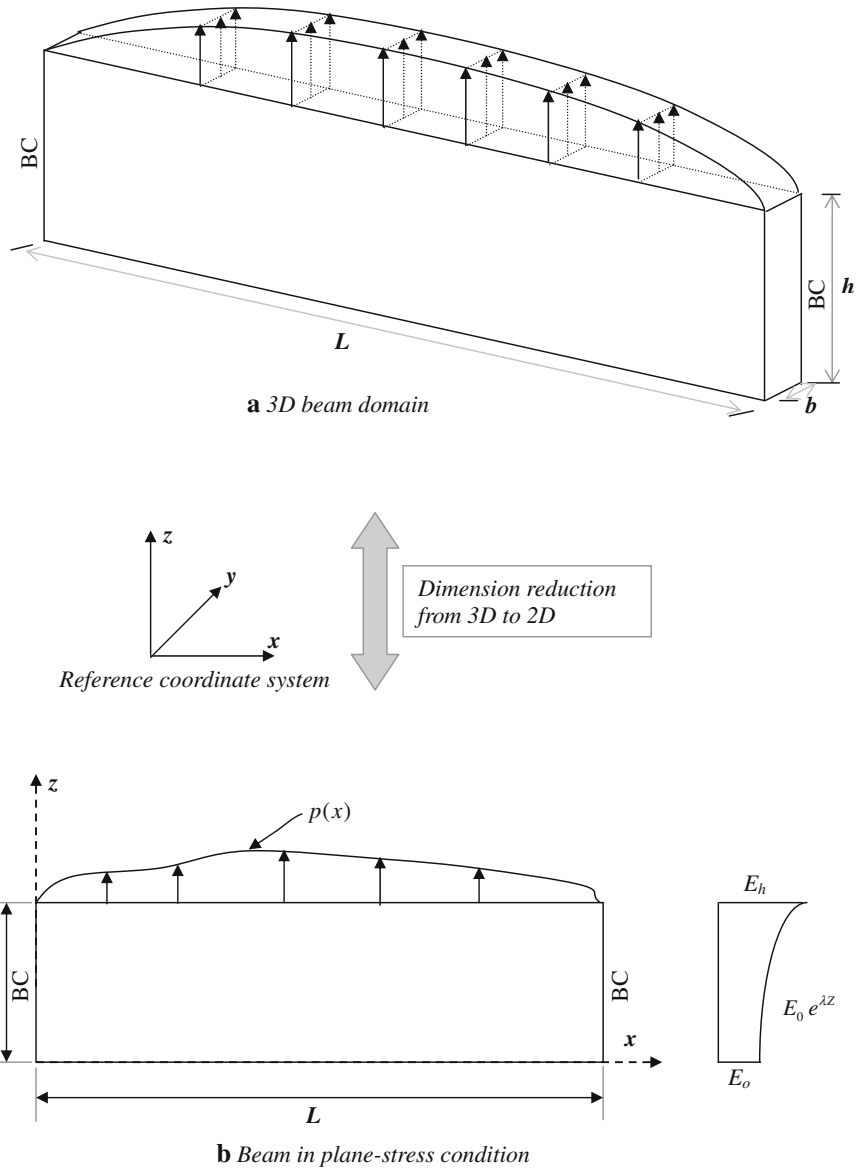

Fig. 1 FG beam subjected to transverse loading

The 2D equations of equilibrium are,

$$\begin{aligned}\frac{\partial \sigma_x}{\partial x}+\frac{\partial \tau_{xz}}{\partial z}+B_x=0\\ \frac{\partial \tau_{zx}}{\partial x}+\frac{\partial \sigma_z}{\partial z}+B_z=0\end{aligned} \tag{2}$$

where, B_x and B_z are the body forces per unit volume in x and z directions, respectively and from the linear theory of elasticity, the strain–displacement relations in 2D are,

$$\varepsilon_x=\frac{\partial u}{\partial x};\quad \varepsilon_z=\frac{\partial w}{\partial z}\quad \text{and}\quad \gamma_{xz}=\frac{\partial u}{\partial z}+\frac{\partial w}{\partial x} \tag{3}$$

It is assumed here that the FG material is isotropic at every point. Further it is assumed that the Poisson's ratio is constant through the thickness of the beam. The variation of the Young's modulus through the thickness of beam is given by $E(z)=E_o e^{\lambda z}$. Therefore, the material constitutive relations for FG beam under plane stress condition can be written as,

$$\begin{Bmatrix}\sigma_x\\ \sigma_z\\ \tau_{xz}\end{Bmatrix}=\begin{bmatrix}C_{11} & C_{12} & 0\\ C_{21} & C_{22} & 0\\ 0 & 0 & C_{33}\end{bmatrix}\begin{Bmatrix}\varepsilon_x\\ \varepsilon_z\\ \gamma_{xz}\end{Bmatrix} \tag{4}$$

The reduced material coefficients, C_{ij} for a FG beam are,

$$C_{11}=C_{22}=\frac{E_o e^{\lambda z}}{(1-\upsilon^2)}\,C_{12}=C_{21}=\frac{\upsilon E_o e^{\lambda z}}{(1-\upsilon^2)}$$
$$\text{and}\quad C_{33}=\frac{E_o e^{\lambda z}}{2(1+\upsilon)}$$

where λ is the $-\ln\frac{E_0}{E_h}$ = Gradation factor, E_0 is the Young's modulus at the bottom of the beam, E_h is the Young's modulus at the top of the beam and υ is the Poisson's ratio.

2.1 Mixed semi analytical model

An attempt is made here to extend a simple, semi-analytical mathematical model developed by Kant et al. (2007a) for stress analysis of FG beams under transverse loads. The semi analytical model is based on defining a two-point BVP governed by a set of coupled first-order ODEs,

$$\frac{\mathrm{d}}{\mathrm{d}z}\mathbf{y}(z)=\mathbf{A}(z)\mathbf{y}(z)+\mathbf{p}(z) \tag{6}$$

in the domain $0<z<h$. Here, $\mathbf{y}(z)$ is an n-dimensional vector of fundamental variables whose number (n) equals the order of PDE/ODE, $\mathbf{A}(z)$ is a $n\times n$ coefficient matrix (which is a function of material properties in thickness direction) and $\mathbf{p}(z)$ is a n-dimensional vector of non-homogenous (loading) terms.

The Eqs. 2–4 have a total of eight unknowns u, w, ε_x, ε_z, γ_{xz}, σ_x, σ_z, τ_{xz} in eight equations. After a simple algebraic manipulation of the above sets of equations, a set of PDEs involving only four primary dependent variables u, w, τ_{zx} and σ_z are obtained as follows,

$$\begin{aligned}\frac{\partial u}{\partial z}&=\frac{\tau_{xz}}{C_{33}}-\frac{\partial w}{\partial x}\\ \frac{\partial w}{\partial z}&=\frac{1}{C_{22}}\left(\sigma_z-C_{21}\frac{\partial u}{\partial x}\right)\\ \frac{\partial \tau_{xz}}{\partial z}&=\left(-C_{11}+\frac{C_{12}C_{21}}{C_{22}}\right)\frac{\partial^2 u}{\partial x^2}-\frac{C_{12}\partial \sigma_z}{C_{22}\,\partial x}-B_x\\ \frac{\partial \sigma_z}{\partial z}&=-\frac{\partial \tau_{xz}}{\partial x}-B_z\end{aligned} \tag{7}$$

A secondary dependent variable, σ_x can be expressed as a function of the primary dependent variables as follows,

$$\sigma_x=C_{11}\frac{\partial u}{\partial x}+C_{12}\frac{\partial w}{\partial z} \tag{8}$$

The above PDEs defined by Eq. 7 can be reduced to a coupled first-order ODEs by using Fourier trigonometric series expansion for primary dependent variables satisfying the simple (diaphragm) support end conditions at $x=0, L$, as follows,

$$\begin{aligned}u(x,z)&=\sum_m u_m(z)\cos\frac{m\pi x}{L}\\ w(x,z)&=\sum_m w_m(z)\sin\frac{m\pi x}{L}\end{aligned} \tag{9}$$

and from the basic relations of theory of elasticity, it can be shown that,

$$\begin{aligned}\tau_{xz}(x,z)&=\sum_m \tau_{xzm}(z)\cos\frac{m\pi x}{L}\\ \sigma_z(x,z)&=\sum_m \sigma_{zm}(z)\sin\frac{m\pi x}{L}\end{aligned} \tag{10}$$

Table 1 Transformation of BVP into IVPs

Intg. no.	Starting edge; z = 0				Final edge; z = h				Load term
	u	w	τ_{xz}	σ_z	u	w	τ_{xz}	σ_z	
1	(assumed) 0	(assumed) 0	(known) 0	(known) 0	Y_{11}	Y_{21}	Y_{31}	Y_{41}	Include
2	(unity) 1	(assumed) 0	0	0	Y_{12}	Y_{22}	Y_{32}	Y_{42}	Exclude
3	(assumed) 0	(unity) 1	0	0	Y_{13}	Y_{23}	Y_{33}	Y_{43}	Exclude
Final	X_1	X_2	Known	Known	u_h	w_h	0	p_{om}	Include

Substituting Eqs. 9–10 into Eq. 7 and noting orthogonality conditions of trigonometric functions, the following ODEs are obtained,

$$\begin{aligned}
\frac{du_m(z)}{dz} &= -\frac{m\pi}{L}w_m(z) + \frac{1}{C_{33}}\tau_{xzm}(z)\\
\frac{dw_m(z)}{dz} &= \frac{C_{21}m\pi}{C_{22}\ L}u_m(z) + \frac{1}{C_{22}}\sigma_{zm}(z)\\
\frac{d\tau_{xzm}(z)}{dz} &= \left(C_{11} - \frac{C_{12}C_{21}}{C_{22}}\right)\frac{m^2\pi^2}{L^2}u_m(z)\\
&\quad - \frac{C_{12}m\pi}{C_{22}\ L}\sigma_{zm}(z) - B_x(x,z)\\
\frac{d\sigma_{zm}(z)}{dz} &= \frac{m\pi}{L}\tau_{xzm}(z) - B_z(x,z)
\end{aligned} \tag{11}$$

Equation 11 represents the governing two-point BVP in ODEs in the domain $0 < z < h$ with stress components known at the top and bottom surfaces (boundary conditions) of the beam. The basic approach to the numerical integration of the BVP defined in Eq. 11 is to transform the given BVP into a set of initial value problems (IVPs)- one non-homogeneous and $n/2$ homogeneous. The solution of BVP defined by Eq. 11 is obtained by forming a linear combination of one non-homogeneous and $n/2$ homogeneous solutions so as to satisfy the boundary conditions at $z = 0$ and h (Kant and Ramesh 1981). This gives rise to a system of $n/2$ linear algebraic equations, the solution of which determines the unknown $n/2$ components, X_1 and X_2 (Table 1) at the starting edge $z = 0$. Then a final numerical integration of Eq. (11) produces the desired results. Displacement and stress boundary conditions on the four edges of the 2D beam are detailed in Table 2.

2.2 Analytical models based on FOST and HOSNT

In order to approximate a 2D elasticity problem to a one dimensional (1D) beam problem, the displacement components $u(x, z)$and $w(x, z)$ at any point in the beam are expanded in Taylor's series in terms of thickness coordinate. The first-order and higher-order displacement fields considered here in the formulation are,

Table 2 Boundary conditions (BCs)

Edge	BCs on displacement field	BCs on stress field
$x = 0, L$	$w = 0$	$\sigma_x = 0$
$x = L/2$	$u = 0$	$\tau_{xz} = 0$
$z = 0$	–	$\sigma_z = 0$; $\tau_{xz} = 0$
$z = h$	–	$\sigma_z = p_{0m}$; $\tau_{xz} = 0$

First-order shear deformation theory (FOST)

$$\begin{aligned}
u(x,z) &= u_o(x) + z\theta_x(x)\\
w(x,z) &= w_o(x)
\end{aligned} \tag{12}$$

Higher-order shear-normal deformation theory (HOSNT)

$$\begin{aligned}
u(x,z) &= u_o(x) + z\theta_x(x) + z^2u_o^*(x) + z^3\theta_x^*(x)\\
w(x,z) &= w_o(x) + z\theta_z(x) + z^2w_o^*(x) + z^3\theta_z^*(x)
\end{aligned} \tag{13}$$

The parameters u_o, w_o, θ_x are the physical one dimensional terms in Taylor's series. The parameters u_0^*, w_o^*, θ_x^*, θ_z, θ_z^* are higher-order terms in Taylor's series expansion and they represent higher-order transverse cross sectional deformations.

In this section, analytical formulation and solution using HOSNT are only presented in detail.

By substitution of the displacement relations given by Eq. 13 into strain–displacement relations (Eq. 3), the following relations are obtained.

$$\begin{aligned}
\varepsilon_x &= \varepsilon_{xo} + z\chi_x + z^2\varepsilon_{xo}^* + z^3\chi_x^*\\
\varepsilon_z &= \varepsilon_{zo} + z\chi_z + z^2\varepsilon_{zo}^*\\
\gamma_{xz} &= \phi_x + z\chi_{xz} + z^2\phi_x^* + z^3\chi_{xz}^*
\end{aligned} \tag{14}$$

where,

$$
\begin{aligned}
(\varepsilon_{xo}, \varepsilon^*_{xo}) &= \left(\frac{du_o}{dx}, \frac{du^*_o}{dx}\right)\\
(\varepsilon_{zo}, \varepsilon^*_{zo}) &= (\theta_z, 3\theta^*_z)\\
(\chi_x, \chi^*_x) &= \left(\frac{d\theta_x}{dx}, \frac{d\theta^*_x}{dx}\right)\\
(\chi_z, \chi_{xz}, \chi^*_{xz}) &= \left(2w^*_o, 2u^*_o + \frac{d\theta_z}{dx}, \frac{d\theta^*_z}{dx}\right)\\
(\phi_x, \phi^*_x) &= \left(\theta_x + \frac{dw_o}{dx}, 3\theta^*_x + \frac{dw^*_o}{dx}\right)
\end{aligned} \tag{15}
$$

2.3 Equilibrium equations and boundary conditions

The governing equations of equilibrium for the stress analysis are obtained using the principle of minimum potential energy (PMPE), which states that for equilibrium, the total potential energy must be stationary. In analytical form it can be written as follows,

$$\delta(U - W_s - W_e) = 0 \tag{16}$$

where, U is the Strain energy of the FG beam, W_s is the Work done by body and surface tractions and W_e is the Work done by edge forces.

The individual terms of the above equation are evaluated as follows.

The virtual strain energy is given by,

$$\delta U = \int_x \int_z \left(\sigma_x \delta\varepsilon_x + \sigma_z \delta\varepsilon_z + \tau_{xz}\delta\gamma_{xz}\right) dxdz \tag{17}$$

Work done by externally applied load can be calculated by,

$$\delta W_s = \int_x p^h_z \delta w^h \, dx \tag{18}$$

where w^h is the transverse displacement at any point on top surface of the beam and is given by

$$\delta w^h = \delta w_o + h\delta\theta_z + h^2\delta w^*_o + h^3\delta\theta^*_z \tag{19}$$

The work done by the edge stresses is given by

$$\delta W_e = \int_z \left(\overline{\sigma}_x \delta u + \overline{\tau}_{xz}\delta w\right) dz \tag{20}$$

in which $\bar{\sigma}_x$ and $\bar{\tau}_{xz}$ are edge stresses at $x = 0$ and L.

By substituting Eqs. 17–20 in the virtual work Eq. 16, and by expressing strains in terms of displacements and integrating through the thickness, a new set of quantities, called stress resultants, defined on the reference axis x and as described in the next section are obtained. Setting the coefficients of $\delta u_o, \delta w_o, \delta\theta_x, \delta\theta_z, \delta u^*_o, \delta w^*_o, \delta\theta^*_x, \delta\theta^*_z$ equal to zero, the following equilibrium equations and boundary conditions are obtained.

The equilibrium equations are:

$$
\begin{aligned}
\delta u_o &: \frac{dN_x}{dx} = 0\\
\delta w_o &: \frac{dQ_x}{dx} + p^h_z = 0\\
\delta\theta_x &: \frac{dM_x}{dx} - Q_x = 0\\
\delta\theta_z &: \frac{dS_x}{dx} - N_z + h(p^h_z) = 0\\
\delta u^*_o &: \frac{dN^*_x}{dx} - 2S_x = 0\\
\delta w^*_o &: \frac{dQ^*_x}{dx} - 2M_z + h^2(p^h_z) = 0\\
\delta\theta^*_x &: \frac{dM^*_x}{dx} - 3Q^*_x = 0\\
\delta\theta^*_z &: \frac{dS^*_x}{dx} - 3N^*_z + h^3(p^h_z) = 0
\end{aligned} \tag{21}
$$

and the boundary conditions are:

$$
\begin{array}{l} N_x = \bar{N}_x \text{or} u_o = \bar{u}_o \\ M_x = \bar{M}_x \text{ or } \theta_x = \bar{\theta}_x \\ N^*_x = \bar{N}^*_x \text{ or } u^*_o = \bar{u}^*_o \\ M^*_x = \bar{M}^*_x \text{ or } \theta^*_x = \bar{\theta}^*_x \end{array} \text{ and } \begin{array}{l} Q_x = \bar{Q}_x \text{ or } w_o = \bar{w}_o \\ S_x = \bar{S}_x \text{ or } \theta_z = \bar{\theta}_z \\ Q^*_x = \bar{Q}^*_x \text{ or } w^*_o = \bar{w}^*_o \\ S^*_x = \bar{S}^*_x \text{ or } \theta^*_z = \bar{\theta}^*_z \end{array} \tag{22}
$$

The bar refers to edge values.

2.4 Stress resultants

The 1D stress resultants in the governing Eqs. 21 and 22 are defined as,

$$
\begin{aligned}
\begin{bmatrix} N_x & M_x & N^*_x & M^*_x \\ N_z & M_z & N^*_z & 0 \end{bmatrix} &= \int_0^h \begin{Bmatrix} \sigma_x \\ \sigma_z \end{Bmatrix} \begin{bmatrix} 1 & z & z^2 & z^3 \end{bmatrix} dz\\
&= \int_o^h \begin{bmatrix} C_{11} & C_{12} \\ C_{21} & C_{22} \end{bmatrix} \begin{Bmatrix} \varepsilon_x \\ \varepsilon_z \end{Bmatrix} \begin{bmatrix} 1 & z & z^2 & z^3 \end{bmatrix} dz
\end{aligned} \tag{23}
$$

and,

$$
\begin{aligned}
\begin{bmatrix} Q_x & S_x & Q^*_x & S^*_x \end{bmatrix} &= \int_o^h \tau_{xz} \begin{bmatrix} 1 & z & z^2 & z^3 \end{bmatrix} dz\\
&= \int_o^h C_{33}\gamma_{xz} \begin{bmatrix} 1 & z & z^2 & z^3 \end{bmatrix} dz
\end{aligned} \tag{24}
$$

Upon integration, these expressions are rewritten in the matrix form as given below.

$$\begin{Bmatrix} N_x \\ M_x \\ N_x^* \\ M_x^* \\ N_z \\ M_z \\ N_z^* \end{Bmatrix}_{7x1} = [A]_{7x7} \begin{Bmatrix} \varepsilon_{xo} \\ \chi_x \\ \varepsilon_{xo}^* \\ \chi_x^* \\ \varepsilon_{zo} \\ \chi_z \\ \varepsilon_{zo}^* \end{Bmatrix}_{7x1} \tag{25}$$

and,

$$\begin{Bmatrix} Q_x \\ S_x \\ Q_x^* \\ S_x^* \end{Bmatrix}_{4x1} = [D]_{4x4} \begin{Bmatrix} \phi_x \\ \chi_{xz} \\ \phi_x^* \\ \chi_{xz}^* \end{Bmatrix}_{4x1} \tag{26}$$

in which, [A] and [D] are the coupled axial-bending and shear stiffness matrices, respectively of the FG beam whose elements are defined in the Appendix.

2.5 Closed-form solution

Navier's solution technique using the Fourier series is used to obtain closed form solution of the 1D beam problem. All displacements and loads acting on the FG beam are defined in terms of Fourier series. The equilibrium equations are solved for displacement amplitudes by substituting stress resultants in terms of displacements expanded in Fourier series.

For the simply (diaphragm) supported boundary conditions, viz.,

$$\begin{matrix} N_x = 0 \\ M_x = 0 \\ N_x^* = 0 \\ M_x^* = 0 \end{matrix} \quad \text{and} \quad \begin{matrix} w_o = 0 \\ \theta_z = 0 \\ w_o^* = 0 \\ \theta_z^* = 0 \end{matrix} \tag{27}$$

The displacements can be expressed in the following forms.

$$\begin{matrix} u_o = \sum_{n=1}^{\infty} u_{on} \cos\frac{n\pi x}{L} \\ \theta_x = \sum_{n=1}^{\infty} \theta_{xn} \cos\frac{n\pi x}{L} \\ u_o^* = \sum_{n=1}^{\infty} u_{on}^* \cos\frac{n\pi x}{L} \\ \theta_x^* = \sum_{n=1}^{\infty} \theta_{xn}^* \cos\frac{n\pi x}{L} \end{matrix} \quad \text{and} \quad \begin{matrix} w_o = \sum_{n=1}^{\infty} w_{on} \sin\frac{n\pi x}{L} \\ \theta_z = \sum_{n=1}^{\infty} \theta_{zn} \sin\frac{n\pi x}{L} \\ w_o^* = \sum_{n=1}^{\infty} w_{on}^* \sin\frac{n\pi x}{L} \\ \theta_z^* = \sum_{n=1}^{\infty} \theta_{zn}^* \sin\frac{n\pi x}{L} \end{matrix} \tag{28}$$

where $u_{on}, \theta_{xn}, u_{on}^*, \ldots\ldots\ldots$.are called displacement Fourier amplitudes. Only odd values of $n = 1, 3, 5, \ldots$ are taken for the assumed transverse load.

The following steps are taken to obtain the required system of equilibrium equations (Eq. 21) in terms of displacements.

1. Eqs. 25–28 are substituted in Eq. 21.
2. The eight equilibrium equations are multiplied with $\cos\frac{m\pi x}{L}$, $\sin\frac{m\pi x}{L}$, $\cos\frac{m\pi x}{L}$, $\sin\frac{m\pi x}{L}$, $\cos\frac{m\pi x}{L}$, $\sin\frac{m\pi x}{L}$,$\cos\frac{m\pi x}{L}$ and $\sin\frac{m\pi x}{L}$, respectively and then integrated between the limits $0 < x < L$.

After following the above two steps with use of orthogonality conditions for trigonometric functions and collecting the displacement coefficients, one obtains:

$$[X]_{8x8} \begin{Bmatrix} u_{on} \\ w_{on} \\ \theta_{xn} \\ \theta_{zn} \\ u_{on}^* \\ w_{on}^* \\ \theta_{xn}^* \\ \theta_{zn}^* \end{Bmatrix}_{8x1} = \begin{Bmatrix} 0 \\ p_z^+ \\ 0 \\ h(p_z^+) \\ 0 \\ h^2(p_z^+) \\ 0 \\ h^3(p_z^+) \end{Bmatrix}_{8x1} \tag{29}$$

for any value of n. The elements of the coefficient matrix $[X]$ are listed in Appendix.

The Fourier amplitudes are obtained by solving Eq. 29. The Fourier displacement amplitudes are then used to calculate the generalized displacement components and their derivatives. The values of generalized displacement components and their derivatives are then substituted in Eqs. 25–26 to obtain the values of stress resultants. The same displacement values are also back substituted into the strain–displacement relations (Eq. 3) to obtain the values of strain. The material constitutive relations (Eq. 4) are then used to compute the in-plane and transverse stresses.

3 Numerical investigation

A computer code is developed by incorporating the present mixed semi analytical, FOST, HOSNT and 2D plane stress elasticity formulations in FORTRAN 90 for the analysis of FG beams under transverse loads. Numerical investigations on two simply supported narrow beams with plane stress condition are performed to establish the accuracy of the models presented in the preceding sections of the paper. The

obtained exact solution based on the 2D plane stress elasticity formulation following Sankar (2001) is considered as benchmark solution for comparison. A shear correction factor of 5/6 is used in computing results using FOST model. The percentage error in results is calculated as,

$$\text{Percentage error} = \left[\frac{\text{Present value} - \text{Elasticity value}}{\text{Elasticity value}}\right] \times 100 \tag{30}$$

and reported as such in all tables.

Following normalizations are used here for the uniform comparison of the results.

$$\begin{aligned} \overline{u} &= \frac{E_h u(0,z)}{p_0 h}; \quad \overline{w} = \frac{100 E_h h^3 w(L/2,z)}{p_0 L^4} \\ \overline{\sigma_x} &= \frac{\sigma_x(L/2,z)}{p_0 L^2}; \quad \overline{\tau_{xz}} = \frac{\tau_{xz}(0,z)}{p_0 L}; \quad \overline{\sigma_z} = \frac{\sigma_z}{p_0} \end{aligned} \tag{31}$$

in which a bar over the variable defines its normalized value. The following set of material properties are used:

Material set 1 (Reddy 2000)

$E_o = 70$ GPa (Aluminum), $E_h = 151$ GPa (Zirconia), $\upsilon = 0.3$.

Material set 2 (Sankar 2001)

$E_o = 1$ GPa, $E_h/E_o = 5$, 10, 20 and 40, $\upsilon = 0.3$.

3.1 Example 1

A simply supported FG beam under sinusoidal load is considered here to show the effectiveness of newly developed mixed semi analytical model over the other simplified models. Material set 1 is used. The normalized inplane normal stress ($\overline{\sigma_x}$), transverse shear stress ($\overline{\tau_{xz}}$) and transverse displacement ($\overline{w}$) for different aspect ratios are presented in Table 3. Moreover, through thickness variations of inplane and transverse displacements ($\overline{u}$ and $\overline{w}$) as well as inplane normal and transverse shear stresses ($\overline{\sigma_x}$ and $\overline{\tau_{xz}}$) for an aspect ratio of 5 are depicted in Fig. 2. The exact elasticity solution and analytical solutions (FOST and HOSNT) are used for comparison. From Table 3, it is clearly seen that the present semi analytical results are exactly matching with the elasticity solution. This proves the superiority of the present mixed model. It is also observed that results obtained by the HOSNT are in good agreement with elasticity solution specially for the slender beam with aspect ratio equal to or greater than 10 whereas, values predicted by FOST differ considerably. The accuracy of both the models, FOST and HOSNT, increases with the increase in aspect ratio.

3.2 Example 2

A simply supported FG beam under sinusoidal transverse load with various gradation factor (λ) is considered further to study the effect of the gradation factor. Material set 2 is used. The normalized inplane normal stress ($\overline{\sigma_x}$), transverse shear stress ($\overline{\tau_{xz}}$) and transverse displacement ($\overline{w}$) for different aspect ratios and different gradation factors ($\lambda = 5$, 10, 20 and 40)

Table 3 Normalized stresses ($\overline{\sigma_x}, \overline{\tau_{xz}}$) and the transverse displacement ($\overline{w}$) of FG beam under sinusoidal transverse load

Variables	L/h	Elasticity solution	Semi analytical solution	HOSNT	FOST
$\overline{\sigma_x}\left(\frac{L}{2}, h\right)$	2	0.8931	0.8931 (.000)	0.9068 (1.534)	0.7833 (−12.294)
	5	0.7972	0.7972 (.000)	0.7995 (.289)	0.7833 (−1.744)
	10	0.7866	0.7866 (.000)	0.7872 (.076)	0.7833 (−.419)
	50	0.7835	0.7835 (.000)	0.7835 (.000)	0.7833 (−.023)
$\overline{\tau_{xz}}(0, \max)$	2	0.4750	0.4746 (−.084)	0.4725 (−.119)	0.4818 (1.432)
	5	0.4800	0.4800 (.000)	0.4801 (.021)	0.4818 (0.375)
	10	0.4810	0.4810 (.000)	0.4813 (.062)	0.4818 (0.166)
	50	0.4814	0.4814 (.000)	0.4818 (.083)	0.4818 (.083)
$\overline{w}\left(\frac{L}{2}, h\right)$	2	30.2430	30.2430 (.000)	30.2071 (−.119)	27.8705 (−7.845)
	5	19.7790	19.7790 (.000)	19.7767 (−.116)	18.7563 (−5.171)
	10	18.5679	18.5679 (.000)	18.5675 (−.002)	18.2041 (−1.959)
	50	18.1957	18.1957 (.000)	18.1957 (.000)	18.1736 (−.121)

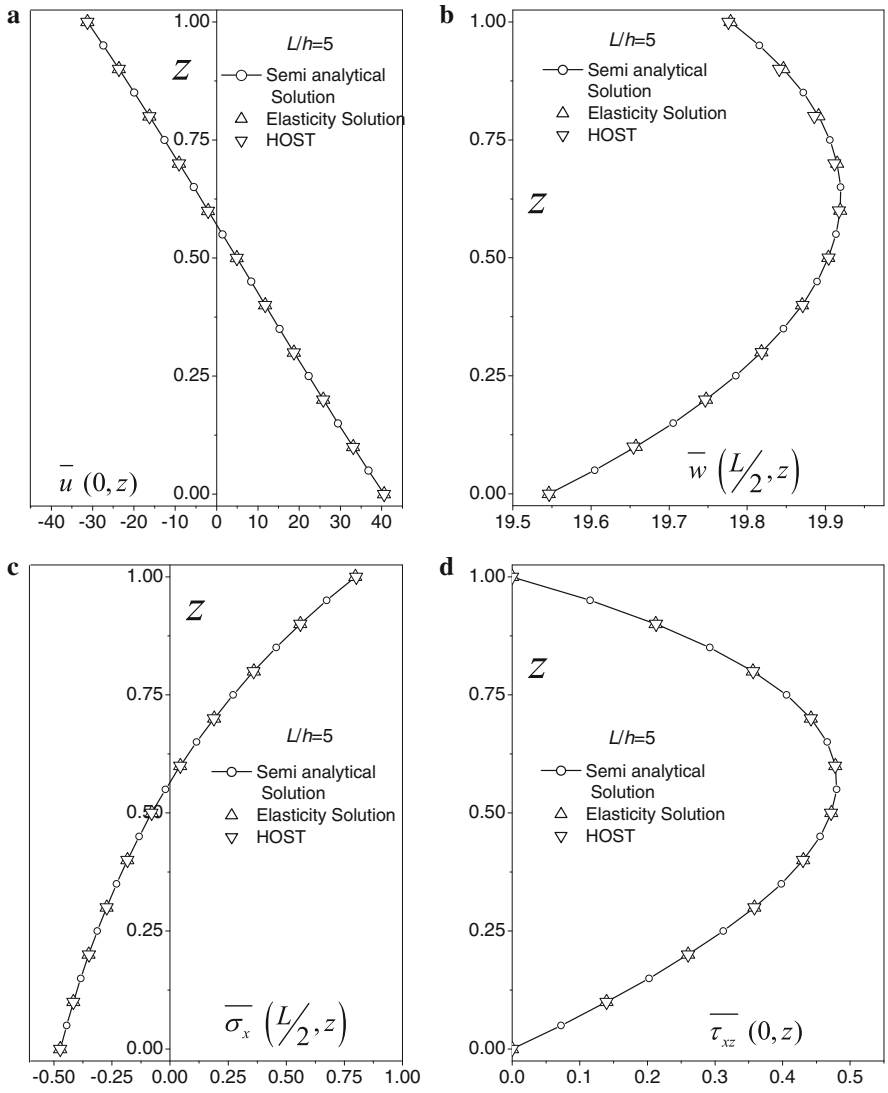

Fig. 2 Through thickness variation of (**a**) inplane displacement $\overline{u}$, (**b**) transverse displacement $\overline{w}$, (**c**) inplane normal stress $\overline{\sigma_x}$ and (**d**) transverse shear stress $\overline{\tau_{xz}}$ for simply supported FG beam under sinusoidal load

are detailed in Tables 4, 5, 6, respectively. Through thickness variations of inplane displacement ($\overline{u}$), transverse displacements ($\overline{w}$), inplane normal stress ($\overline{\sigma_x}$) and transverse shear stress ($\overline{\tau_{xz}}$) for an aspect ratio of 5 are shown in Fig. 3. The 2D elasticity, FOST and HOSNT solutions are used for comparison. It can be concluded from the results contained in Tables 4, 5, 6 that the present mixed semi analytical model works well for any variation of Young's modulus whereas, 1D shear deformation beam models (FOST and HOSNT) do not seems to give consistent estimates. No consistency in the variation of percentage errors in HOSNT and FOST models with increase in gradation factor is observed for all the values. This observation clearly reinforces the stability, consistency, reliability and accuracy of mixed semi analytical model over FOST and HOSNT 1D beam models.

3.3 Example 3

A simply supported FG beam loaded with uniformly distributed load is considered here to show the ability of all developed formulations to handle different loading conditions. Material set 2 is used. The ratio of Young's modulus of top fiber to bottom fiber (λ) is taken as 5. The normalized inplane normal stress ($\overline{\sigma_x}$), transverse shear stress ($\overline{\tau_{xz}}$) and transverse displacement ($\overline{w}$) for different aspect ratios are presented in Table 7. The 2D exact elasticity solution

Table 4 Normalized inplane normal stresses ($\overline{\sigma_x}$) of FG beam under sinusoidal transverse load with different gradation factors

L/h	E_h/E_0	Elasticity solution	Semi analytical solution	HOSNT	FOST
2	5	1.1861	1.1861 (.000)	1.1999 (1.163)	1.0290 (−13.245)
	10	1.4912	1.4912 (.000)	1.5039 (.852)	1.2858 (−13.774)
	20	1.8640	1.8640 (.000)	1.8746 (.569)	1.6035 (−13.975)
	40	2.3138	2.3138 (.000)	2.3219 (.350)	1.9939 (−13.826)
5	5	1.0507	1.0507 (−.000)	1.0530 (.219)	1.0290 (−2.065)
	10	1.3157	1.3157 (.000)	1.3176 (.144)	1.2858 (−2.273)
	20	1.6429	1.6429 (.000)	1.6443 (.085)	1.6035 (−2.398)
	40	2.0437	2.0437 (.000)	2.0444 (.034)	1.9939 (−2.437)
10	5	1.0343	1.0343 (.000)	1.0349 (.058)	1.0290 (−.512)
	10	1.2932	1.2932 (.000)	1.2936 (.031)	1.2858 (−.572)
	20	1.6132	1.6132 (.000)	1.6136 (.025)	1.6035 (−.601)
	40	2.0063	2.0063 (.000)	2.0065 (.010)	1.9939 (−.618)

Values reported in the table are at the center of beam ($L/2$) and at a top surface (h)

Table 5 Normalized transverse stresses ($\overline{\tau_{xz}}$) of FG beam under sinusoidal transverse load with different gradation factors

L/h	E_h/E_0	Elasticity solution	Semi analytical solution	HOSNT	FOST
2	5	0.4971	0.4971 (.000)	0.4942 (−.503)	0.4966 (−.020)
	10	0.5246	0.5246 (.000)	0.5220 (−.496)	0.5169 (−1.468)
	20	0.5606	0.5606 (.000)	0.5579 (−.482)	0.5451 (−2.765)
	40	0.6043	0.6043 (.000)	0.6014 (−.480)	0.5809 (−3.872)
5	5	0.4960	0.4960 (−.000)	0.4957 (−.060)	0.4966 (.121)
	10	0.5166	0.5166 (.000)	0.5172 (.116)	0.5169 (.058)
	20	0.5451	0.5451 (.000)	0.5465 (.257)	0.5441 (−.183)
	40	0.5843	0.5843 (.000)	0.5838 (−.086)	0.5809 (−.582)
10	5	0.4954	0.4954 (.000)	0.4964 (.202)	0.4966 (.242)
	10	0.5156	0.5156 (.000)	0.5170 (.272)	0.5167 (.213)
	20	0.5441	0.5441 (.000)	0.5454 (.239)	0.5451 (.184)
	40	0.5817	0.5817 (.000)	0.5816 (−.017)	0.5809 (−.138)

Values reported in the table are the maximum values at the end of beam ($x = 0$)

Table 6 Normalized transverse displacement ($\overline{w}$) of FG beam under sinusoidal transverse load with different gradation factors

L/h	E_h/E_0	Elasticity solution	Semi analytical solution	HOSNT	FOST
2	5	45.7170	45.7170 (.000)	45.6550 (−.136)	41.4500 (−9.334)
	10	63.9108	63.9108 (.000)	63.8126 (−.154)	56.9027 (−10.965)
	20	88.6534	88.6537 (.000)	88.5046 (−.168)	77.5026 (−12.578)
	40	121.7450	121.7450 (.000)	121.5370 (−.171)	104.8031 (−13.916)
5	5	30.5457	30.5457 (−.000)	30.5379 (−.026)	28.0945 (−8.025)
	10	43.7268	43.7268 (.000)	43.7094 (−.040)	39.9184 (−8.710)
	20	62.3710	62.3710 (.000)	62.3397 (−.050)	56.5685 (−9.303)
	40	88.3008	88.3008 (.000)	88.2526 (−.055)	79.6864 (−9.756)
10	5	28.6816	28.6816 (.000)	28.6798 (−.006)	26.3866 (−8.002)
	10	41.1518	41.1518 (.000)	41.1474 (−.011)	37.6920 (−8.407)
	20	58.9157	58.9157 (.000)	58.9076 (−.014)	53.5780 (−9.090)
	40	83.7957	83.7957 (.000)	83.7831 (−.015)	76.0982 (−9.186)

Values reported in the table are at the center of beam ($L/2$) and at a top surface (h)

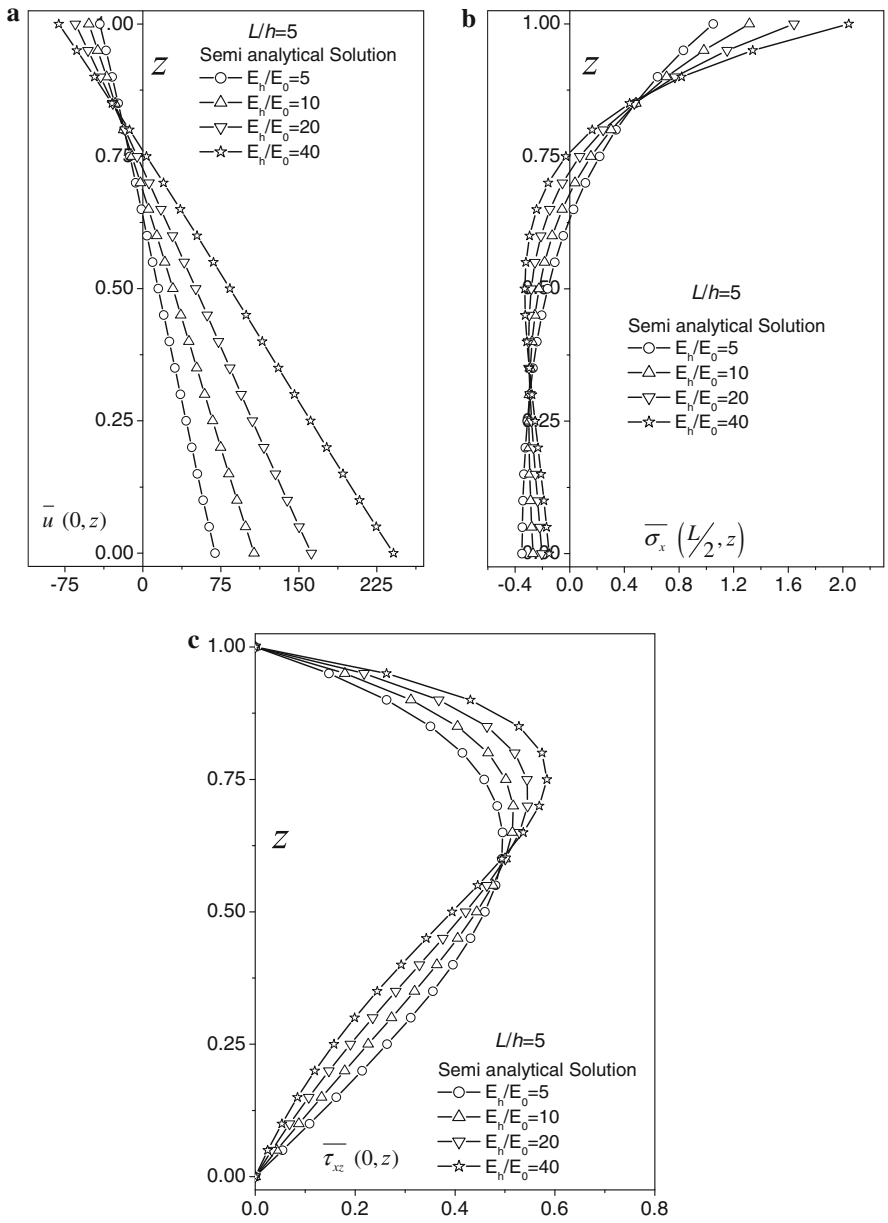

Fig. 3 Through thickness variation of (**a**) inplane displacement $\overline{u}$, (**b**) inplane normal stress $\overline{\sigma_x}$ and (**c**) transverse shear stress $\overline{\tau_{xz}}$ for simply supported FG beam under sinusoidal load

and the 1D analytical FOST and HOSNT beam solutions are used for comparison. Convergence study is performed to estimate the number of harmonics required to define uniformly distributed load. About 13-15 harmonics are required for converged solutions in case of mixed semi-analytical model whereas large number of harmonics is required for HOSNT and FOST models. From Table 7, it is clearly seen that the percentage errors in the mixed semi-analytical solutions are very less as compared to analytical solutions based on FOST and HOSNT. This again proves the superiority of the present mixed model.

4 Concluding remarks

A simple mixed semi analytical model developed by Kant et al. (2007a) is extended here for 2D stress analysis of FG beam under plane stress condition of elasticity. A two-point BVP governed by a set of coupled first-order ODEs is formed by assuming a

Table 7 Normalized stresses ($\overline{\sigma_x}, \overline{\tau_{xz}}$) and the transverse displacement ($\overline{w}$) of FG beam under uniformly distributed transverse load

Variables	L/h	Elasticity solution	Semi analytical solution	HOSNT	FOST
$\overline{\sigma_x}\left(\frac{L}{2}, h\right)$	2	1.4032	1.4000 (−.228)	1.4191 (1.133)	1.2695 (−9.528)
	5	1.2901	1.2902 (.008)	1.2927 (.202)	1.2695 (−1.597)
	10	1.2746	1.2747 (.008)	1.2753 (.055)	1.2695 (−.400)
$\overline{\tau_{xz}}(0, \max)$	2	0.7534	0.7520 (−.186)	0.7716 (2.416)	0.7747 (2.827)
	5	0.7610	0.7618 (−.105)	0.7711 (1.327)	0.7747 (1.800)
	10	0.7694	0.7686 (−.104)	0.7705 (.143)	0.7747 (0.689)
$\overline{w}\left(\frac{L}{2}, h\right)$	2	56.8642	56.8500 (−.025)	56.8026 (−.108)	52.0221 (−8.515)
	5	38.6410	38.6405 (−.001)	38.6315 (−.025)	35.5455 (−8.011)
	10	36.3563	36.3563 (.000)	36.3540 (−.006)	34.1917 (−5.954)

chosen set of primary variables in the form of trigonometric functions along the longitudinal direction of the beam which satisfy the simply (diaphragm) supported end conditions exactly. No simplifying assumptions through the thickness of the beam are introduced. Exact 2D elasticity solution and analytical solutions based on 1D shear deformation beam theories are also developed for comparison and to show the effectiveness and simplicity of the mixed semi analytical model over the other simplified beam models. The present mixed semi analytical model is relatively simple in mathematical complexity and computational efforts. Further, it is seen to be very effective and highly accurate. The main feature of the mixed semi analytical formulation is that the governing differential equation system is not transformed into an algebraic equation system, thus the intrinsic behavior of the physical system is retained to a greater degree of accuracy.

Appendix

The elements of matrix [A] are,

$$[A] = \int_o^h \begin{bmatrix} C_{11} & zC_{11} & z^2C_{11} & z^3C_{11} & C_{13} & zC_{13} & z^2C_{13} \\ zC_{11} & z^2C_{11} & z^3C_{11} & z^4C_{11} & zC_{13} & z^2C_{13} & z^3C_{13} \\ z^2C_{11} & z^3C_{11} & z^4C_{11} & z^5C_{11} & z^2C_{13} & z^3C_{13} & z^4C_{13} \\ z^3C_{11} & z^4C_{11} & z^5C_{11} & z^6C_{11} & z^3C_{13} & z^4C_{13} & z^5C_{13} \\ C_{13} & zC_{13} & z^2C_{13} & z^3C_{13} & C_{33} & zC_{33} & z^2C_{33} \\ zC_{13} & z^2C_{13} & z^3C_{13} & z^4C_{13} & zC_{33} & z^2C_{33} & z^3C_{33} \\ z^2C_{13} & z^3C_{13} & z^4C_{13} & z^5C_{13} & z^2C_{33} & z^3C_{33} & z^4C_{33} \end{bmatrix} dz$$

$$= A_{ij}(i, j = 1 \text{ to } 7)$$

and the coefficients are,

$$A_{11} = \frac{\bar{E}_h - \bar{E}_o}{\lambda} \quad A_{12} = \frac{h\bar{E}_h - A_{11}}{\lambda}$$

$$A_{13} = \frac{h^2\bar{E}_h - 2A_{12}}{\lambda} \quad A_{14} = \frac{h^3\bar{E}_h - 3A_{13}}{\lambda}$$

$$A_{15} = \upsilon A_{11} \quad A_{16} = \upsilon A_{12} \quad A_{17} = \upsilon A_{13}$$

$$A_{22} = A_{13} \quad A_{23} = A_{14} \quad A_{24} = \frac{h^4\bar{E}_h - 4A_{23}}{\lambda}$$

$$A_{25} = \upsilon A_{21} \quad A_{26} = \upsilon A_{22} \quad A_{27} = \upsilon A_{23}$$

$$A_{33} = A_{24} \quad A_{34} = \frac{h^5\bar{E}_h - 5A_{33}}{\lambda}$$

$$A_{35} = \upsilon A_{31} \quad A_{36} = \upsilon A_{32} \quad A_{37} = \upsilon A_{33}$$

$$A_{44} = \frac{h^6\bar{E}_h - 6A_{43}}{\lambda} \quad A_{45} = \upsilon A_{41} \quad A_{46} = \upsilon A_{42}$$

$$A_{47} = \upsilon A_{43}$$

$$A_{55} = A_{11} \quad A_{56} = A_{12} \quad A_{57} = A_{13}$$

$$A_{66} = A_{22} \quad A_{67} = A_{23} \quad A_{77} = A_{33}$$

where, $\bar{E}_h = \left(\frac{E_o}{1-\upsilon^2}\right)e^{\lambda}$ and $\bar{E}_o = \frac{E_o}{(1-\upsilon^2)}$

and $A_{ij} = A_{ji}$ $(i, j = 1 \text{ to } 7)$

The elements of matrix [D] are,

$$[D] = \int_o^h \begin{bmatrix} C_{44} & zC_{44} & z^2C_{44} & z^3C_{44} \\ zC_{44} & z^2C_{44} & z^3C_{44} & z^4C_{44} \\ z^2C_{44} & z^3C_{44} & z^4C_{44} & z^5C_{44} \\ z^3C_{44} & z^4C_{44} & z^5C_{44} & z^6C_{44} \end{bmatrix} dz$$

$$= D_{ij} \ (i, j = 1 \text{ to } 4)$$

and the coefficients are,

$$D_{11}=\frac{1-\upsilon}{2}A_{11}\quad D_{12}=\frac{1-\upsilon}{2}A_{12}\quad D_{13}=\frac{1-\upsilon}{2}A_{13}$$
$$D_{14}=\frac{1-\upsilon}{2}A_{14}$$
$$D_{22}=\frac{1-\upsilon}{2}A_{22}\quad D_{23}=\frac{1-\upsilon}{2}A_{23}\quad D_{24}=\frac{1-\upsilon}{2}A_{24}$$
$$D_{33}=\frac{1-\upsilon}{2}A_{33}\quad D_{34}=\frac{1-\upsilon}{2}A_{34}$$
$$D_{44}=\frac{1-\upsilon}{2}A_{44}$$

and $D_{ij}=D_{ji}$, $(i, j = 1$ to $4)$

The coefficients of matrix [X] are,

$$X_{11}=A_{11}\left(\frac{m\pi}{L}\right)^2\quad X_{12}=0,\quad X_{13}=A_{12}\left(\frac{m\pi}{L}\right)^2$$
$$X_{14}=-A_{15}\left(\frac{m\pi}{L}\right)\quad X_{15}=A_{13}\left(\frac{m\pi}{L}\right)^2$$
$$X_{16}=-2A_{16}\left(\frac{m\pi}{L}\right)$$
$$X_{17}=A_{14}\left(\frac{m\pi}{L}\right)^2 X_{18}=-3A_{17}\left(\frac{m\pi}{L}\right)$$

$$X_{22}=D_{11}\left(\frac{m\pi}{L}\right)^2\quad X_{23}=D_{11}\left(\frac{m\pi}{L}\right)\quad X_{24}=D_{12}\left(\frac{m\pi}{L}\right)^2$$
$$X_{25}=2D_{12}\left(\frac{m\pi}{L}\right)\quad X_{26}=D_{13}\left(\frac{m\pi}{L}\right)^2$$
$$X_{27}=3D_{13}\left(\frac{m\pi}{L}\right)\quad X_{28}=D_{14}\left(\frac{m\pi}{L}\right)^2$$

$$X_{33}=A_{22}\left(\frac{m\pi}{L}\right)^2+D_{11}\quad X_{34}=(-A_{25}+D_{12})\left(\frac{m\pi}{L}\right)$$
$$X_{35}=A_{23}\left(\frac{m\pi}{L}\right)^2+2D_{12}\quad X_{36}=(-2A_{26}+D_{13})\left(\frac{m\pi}{L}\right)$$
$$X_{37}=A_{24}\left(\frac{m\pi}{L}\right)^2+3D_{13}\quad X_{38}=(-3A_{27}+D_{14})\left(\frac{m\pi}{L}\right)$$

$$X_{44}=A_{55}+D_{22}\left(\frac{m\pi}{L}\right)^2\quad X_{45}=(-A_{53}+2D_{22})\left(\frac{m\pi}{L}\right)$$
$$X_{46}=2A_{56}+D_{23}\left(\frac{m\pi}{L}\right)^2\quad X_{47}=(-A_{54}+3D_{23})\left(\frac{m\pi}{L}\right)$$
$$X_{48}=3A_{57}+D_{24}\left(\frac{m\pi}{L}\right)^2$$

$$X_{55}=A_{33}\left(\frac{m\pi}{L}\right)^2+4D_{22}\quad X_{56}=(-2A_{36}+2D_{23})\left(\frac{m\pi}{L}\right)$$
$$X_{57}=A_{34}\left(\frac{m\pi}{L}\right)^2+6D_{23}\quad X_{58}=(-3A_{37}+2D_{24})\left(\frac{m\pi}{L}\right)$$

$$X_{66}=4A_{66}+D_{33}\left(\frac{m\pi}{L}\right)^2\quad X_{67}=(-2A_{64}+3D_{33})\left(\frac{m\pi}{L}\right)$$
$$X_{68}=6A_{67}+D_{34}\left(\frac{m\pi}{L}\right)^2$$

$$X_{77}=A_{44}\left(\frac{m\pi}{L}\right)^2+9D_{13}\quad X_{78}=(-3A_{47}+3D_{24})\left(\frac{m\pi}{L}\right)$$

$$X_{88}=9A_{77}+D_{44}\left(\frac{m\pi}{L}\right)^2$$

and $X_{ij}=X_{ji}$, $(i,j = 1$ to $8)$

References

Bian, Z.G., Chen, W.Q., Lim, C.W., Zhang, N.: Analytical solution for single and multi span functionally graded plates in cylindrical bending. Int. J. Solids Struct. **42**, 6433–6456 (2005)

Bodaghi, M., Saidi, A.R.: Levy-type solution for bending analysis of thick functionally graded rectangular plates based on the higher-order shear deformation plate theory. Appl. Math. Model. **34**, 3659–3670 (2010)

Chakraborty, A., Gopalakrishnan, S.: A new beam finite element for the analysis of functionally graded materials. Int. J. Mech. Sci. **45**, 519–539 (2003a)

Chakraborty, A., Gopalakrishnan, S.: A spectrally formulated finite element for wave propagation analysis in functionally graded beams. Int. J. Solids Struct. **40**, 2421–2448 (2003b)

Ching, H.K., Chen, J.K.: Thermomechanical analysis of functionally graded composites under laser heating by the MLPG methods. Comput. Model. Eng. Sci. **13**(3), 199–218 (2006)

Han, F., Pan, E., Roy, A.K., Yue, Z.Q.: Response of piezoelectric, transversely isotropic, functionally graded and multilayered half spaces to uniform circular surface loadings. Comput. Model. Eng. Sci. **14**(1), 15–30 (2006)

Kang, Y.A., Li, X.F.: Bending of functionally graded cantilever beam with power-law non-linearity subjected to an end force. Int. J. Non Linear Mech. **44**, 696–703 (2009)

Kant, T.: Numerical analysis of thick plates. Comput. Methods Appl. Mech. Eng. **31**(3), 1–18 (1982)

Kant, T., Manjunatha, B.S.: An unsymmetric FRC laminate C^0 finite element model with 12 degrees of freedom per node. Eng. Comput. **5**(3), 300–308 (1998)

Kant, T., Ramesh, C.K.: Numerical integration of linear boundary value problems in solid mechanics by segmentation method. Int. J. Numer. Methods Eng. **17**, 1233–1256 (1981)

Kant, T., Owen, D.R.J., Zienkiwicz, O.C.: A refined higher-order C^0 plate bending element. Comput. Struct. **15**(2), 177–183 (1982)

Kant, T., Pendhari, S.S., Desai, Y.M.: On accurate stress analysis of composite and sandwich narrow beams. Int. J. Comput. Methods Eng. Sci. Mech. **8**(3), 165–177 (2007a)

Kant, T., Pendhari, S.S., Desai, Y.M.: A general partial discretization methodology for interlaminar stress computation in composite laminates. Comput. Model. Eng. Sci. **17**(2), 135–161 (2007b)

Khabbaz, R.S., Manshadi, B.D., Abedian, A.: Nonliear analysis of FGM Plates under pressure loads using the higher-order shear deformation theories. Composite Struct. **89**, 333–344 (2009)

Koizumi, M.: The concept of FGM. Ceramic transactions. Funct. Gradient Mater. **34**, 3–10 (1993)

Lee, H.J.: Layerwise analysis of thermal shape control in graded piezoelectric beams. ASME Aerosp. Division (Publication) AD **68**, 79–87 (2003)

Matsunaga, H.: Stress analysis of functionally graded plates subjected to thermal and mechanical loading. Composite Struct. **87**, 344–357 (2009)

Nguyen, T.K., Sab, K., Bonnet, G.: First-order shear deformation plate models for functionally graded materials. Compos. Mater. **83**, 25–36 (2008)

Reddy, J.N.: Analysis of functionally graded plates. Int. J. Numer. Methods Eng. **47**, 663–684 (2000)

Sankar, B.V.: An elasticity solution for functionally graded beam. Compos. Sci. Technol. **61**, 689–696 (2001)

Sankar, B.V., Tzeng, J.T.: Thermal stresses in functionally graded beams. AIAA J. **410**(6), 1228–1232 (2002)

Sladek, J., Slasek, V., Zhang, Ch.: The MLPG method for crack analysis in anisotropic functionally graded materials. Struct. Integr. Durab. **1**(2), 131–144 (2005)

Soldatos, K.P., Liu, S.L.: On the generalised plane strain deformations of thick anisotropic composite laminated plates. Int. J. Solids Struct. **38**, 479–482 (2001)

Thomson, W.T.: Transmission of elastic waves through a stratified solid medium. J. Appl. Phys. **21**, 89–93 (1950)

Vel, S.S., Batra, R.C.: Analytical solution for rectangular thick laminated plates subjected to arbitrary boundary conditions. AIAA J. **37**, 1464–1473 (1999)

Woo, J., Meguid, S.A.: Nonlinear analysis of functionally graded plates and shells. Int. J. Solids Struct. **38**, 7409–7421 (2001)

Woo, J., Meguid, S.A., Stranart, J.C., Liew, K.M.: Thermomechanical postbuckling analysis of moderately thick functionally graded plates and shallow shells. Int. J. Mech. Sci. **47**, 1147–1171 (2005)

Yamanouchi, M., Koizumi, M., Shiota, T. Proceedings of the first international symposium on functionally gradient materials, Sendai, Japan (1990)